JOURNAL OF GUIDANCE, CONTROL, AND DYNAMICS
Vol. 32, No. 2, March–April 2009

Designing Trajectories in a Planet–Moon Environment Using the Controlled Keplerian Map

Piyush Grover* and Shane Ross†
Virginia Polytechnic Institute and State University, Blacksburg, Virginia 24060

DOI: 10.2514/1.38320

The design of fuel-efficient trajectories that visit different moons of a planetary system is best handled by breaking the problem up into multiple three-body problems. This approach, called the patched three-body approach, has received considerable attention in recent years and has proved to lead to substantial fuel savings compared with the traditional patched-conic approach. We consider the problem of designing fuel-efficient multimoon orbiter spacecraft trajectories in the Jupiter–Europa–Ganymede spacecraft system with realistic transfer times. First, fuel-optimal (i.e., near-zero-fuel) trajectories without the use of any control are determined, but turn out to be infeasible due to the very long transfer times involved. We then describe a methodology that exploits the underlying structure of the dynamics of the two three-body problems, that is, the Jupiter–Europa spacecraft and Jupiter–Ganymede spacecraft, using the Hamiltonian structure-preserving Keplerian map approximations derived earlier and small control inputs in the form of instantaneous ΔV to get trajectories with times of flight on the order of months rather than several years. A typical trajectory constructed using the control algorithm can complete the mission in about 10% of the time of flight of an uncontrolled trajectory.

I. Introduction

LOW-ENERGY spacecraft trajectories, such as multimoon orbiters for the Jupiter system, can be obtained by harnessing multiple gravity assists by moons in conjunction with ballistic capture to drastically decrease fuel usage [1–3]. These phenomena have been explained by applying techniques from dynamical systems theory to systems of n bodies considered three at a time [4–8]. One can design trajectories with a predetermined future and past, in terms of transfer from one Hill's region to another. Using this approach, which has been dubbed the multimoon orbiter (MMO) [1], a scientific spacecraft can orbit several moons for any desired duration, instead of flybys lasting only seconds. This approach should work well with existing techniques, enhancing interplanetary trajectory design capabilities for missions in planet–moon environments. The approach is quite flexible in the sense that the spacecraft can be made to respond to unforeseen events and can be made to revisit any region.

The aim of this paper is to describe a methodology using the analytically derived Keplerian map [9] to obtain trajectories with a realistic time of flight (i.e., measured in months instead of years) using small control inputs in the form of instantaneous ΔV.

The paper is arranged as follows. We first describe the Keplerian map, which is the analytical tool used in the process of finding desired trajectories. We then review the framework of breaking down the multimoon problem into two three-body problems and describe a method of finding zero-fuel trajectories that go from one moon to the other. Using this framework, we then describe the methodology for generating low-energy trajectories that can be completed in a reasonable time using small control inputs. We also discuss the tradeoff between fuel consumption and time of flight for the family of trajectories obtained using this method.

Received 29 April 2008; revision received 19 August 2008; accepted for publication 21 September 2008.

*Ph.D. Candidate, Department of Engineering Science and Mechanics, 313 Norris Hall, Mail Code 0219.

†Assistant Professor, Department of Engineering Science and Mechanics, 224 Norris Hall, Mail Code 0219.

II. Keplerian Map for Evolution Under Natural Dynamics of the Planar Circular Restricted Three-Body Problem

Each map, which we call the Keplerian map, is an update map for the angle of periapse ω in the rotating frame and Keplerian energy K, $(\omega_n, K_n) \mapsto (\omega_{n+1}, K_{n+1})$. The map has the form

$$\begin{pmatrix} \omega_{n+1} \\ K_{n+1} \end{pmatrix} = \begin{pmatrix} \omega_n - 2\pi\{-2[K_n + \mu f(\omega_n; C_J, \bar{K})]\}^{-3/2} \\ K_n + \mu f(\omega_n; C_J, \bar{K}) \end{pmatrix} \quad (1)$$

that is, a map of the cylinder $\mathcal{A} = S^1 \times \mathbf{R}$ onto itself. This two-dimensional symplectic twist map is an approximation of a Poincaré map of the planar circular restricted three-body problem (PCR3BP), in which the surface of section is at periapsis in the space of orbital elements. For this reason, Eq. (1) could be considered a periapse map. The map models a spacecraft on a near-Keplerian orbit about a central body of unit mass, where the spacecraft is perturbed by a smaller body of mass $\mu \ll 1$ on a circular orbit. The map is valid when the spacecraft is assumed to have a periapse distance larger than the perturber's circular orbit. The interaction of the spacecraft with the perturber is modeled as an impulsive kick at periapsis passage, encapsulated in the kick function f; see Fig. 1a, in which $(\mu, C_J, \bar{K})$ are considered bifurcation parameters. Here C_J is the Jacobian constant, which is numerically equal to twice the CR3BP Hamiltonian in a rotating frame, with an opposite sign by convention. The kick function f multiplied by the mass ratio μ is the change in K between two consecutive periapses.

The kick function, derived elsewhere [9] and given in the Appendix, depends on the following procedure. The greatest perturbation in orbital elements for a spacecraft in this regime of motion is assumed to take place at periapse. The spacecraft motion, during free flight, is mechanically constrained to remain on the CR3BP energy surface. By assuming $C_J \approx 3$ (close to the Jacobian constant of the equilibrium points L_1 and L_2), the total change in K is calculated to the first order in μ by integrating the perturbation term over an unperturbed orbit, from apoapsis to apoapsis, in the case of a periapse map. The integral is calculated numerically by quadrature, assuming an average value of K (called $\bar{K}$) over the region for which the map is being used. Because of the form of the integrals, the resulting function $f(\omega)$ is odd in ω. The kick function $f(\omega)$ can be computed for a specific value of ω during each evaluation of the Keplerian map or it can be computed beforehand and stored for all values of ω.

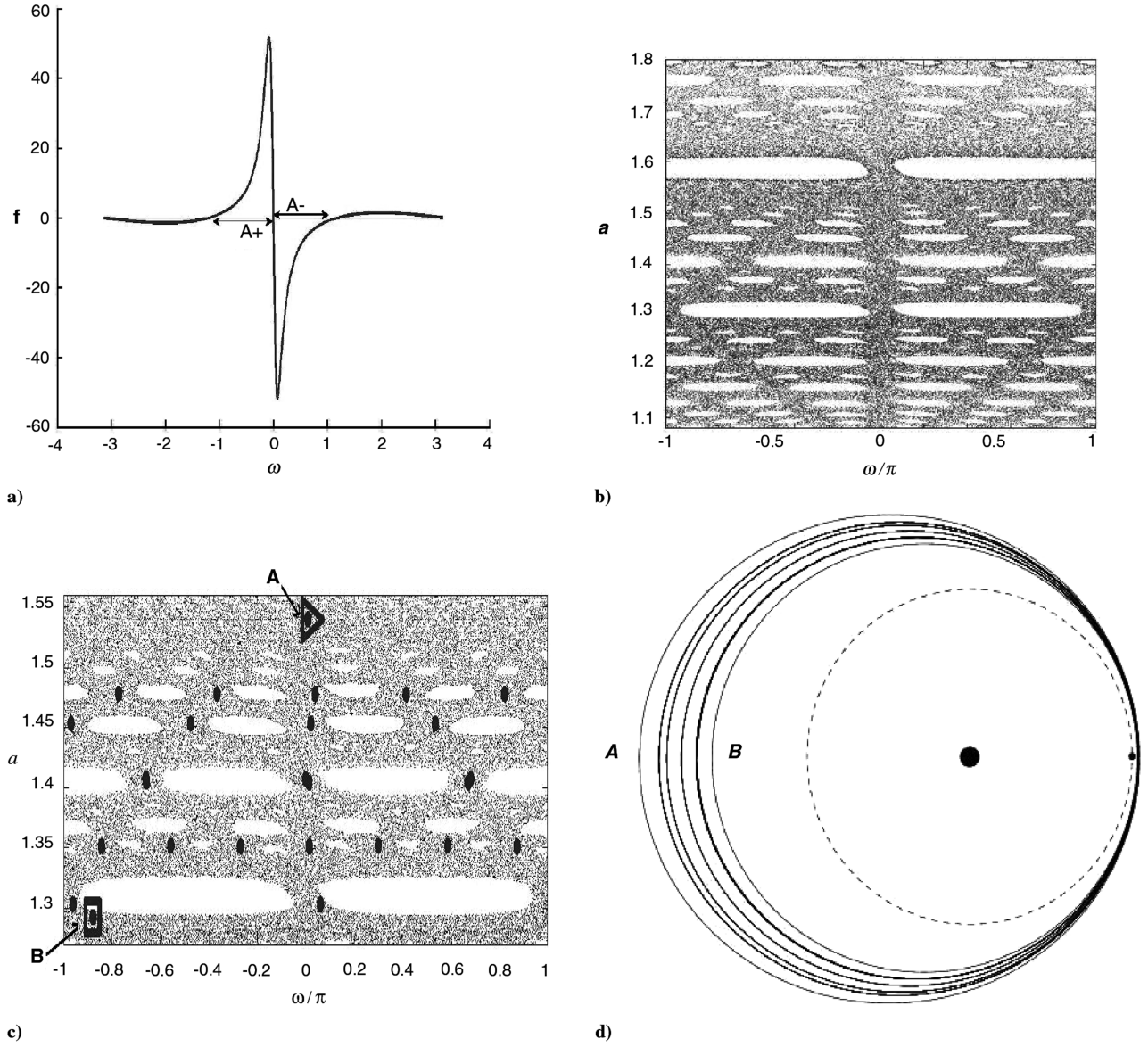

Fig. 1 Shown are the following. a) The energy kick function f vs ω for typical values of the parameters. b) The connected chaotic sea in the phase space of the Keplerian map. The semimajor axis a vs the angle of periapsis ω is shown for parameters $\mu = 5.667 \times 10^{-5}$, $C_J = 2.995$, and $\bar{a} = -1/(2\bar{K}) = 1.35$ appropriate for a spacecraft in the Jupiter–Callisto system. The initial conditions were taken initially in the chaotic sea and followed for 10^4 iterates, thus producing the "swiss cheese" appearance wherein holes corresponding to stable resonant islands reside. c) A phase space trajectory for which the initial point is marked with a triangle and the final point with a square. d) The configuration space projections in an inertial frame for this trajectory. Jupiter and Callisto are shown at their initial positions, and Callisto's orbit is dashed. The uncontrolled spacecraft migration is from larger to smaller semimajor axes, keeping the periapsis direction roughly constant in inertial space. Both the spacecraft and Callisto orbit Jupiter in a counterclockwise sense.

The map effectively captures the dynamics of the full equations of motion; namely, the phase space, shown in Fig. 1b, is densely covered by chains of stable resonant islands, in between which is a connected chaotic zone. The more physically intuitive semimajor axis a is plotted for the vertical axis instead of Keplerian energy K, where $a = -1/(2K)$. The kick function obtained from the map shows that the biggest kicks are received for a very narrow range of periapse angle values. If the periapse occurs slightly ahead of the perturber, the spacecraft gets a negative a kick, and, if the periapse is slightly behind the perturber, the kick is positive. In Fig. 1a, these regions are labeled A_- and A_+ respectively.

Using similar methods as already described, we can construct an apoapse map for the case in which the spacecraft is in the interior realm of the CR3BP, that is, when its apoapse distance is less than the circular orbit of the perturber. In the case of an apoapse map, to receive the positive a kick, the apoapse needs to be slightly ahead of the perturber (or the periapse needs to be slightly less than π). Similarly, for a negative a kick, the apoapse needs to be slightly behind the perturber (or the periapse needs to be slightly more than $-\pi$). Both the periapse and apoapse maps will be referred to as Keplerian maps, and the context should reveal which is being used.

The engineering application envisioned for the map is the design of low-energy trajectories, specifically between moons in the Jupiter moon system. Multiple gravity assists are a key physical mechanism that could be exploited in future scientific missions [1]. For example, a trajectory sent from Earth to the Jovian system, just grazing the orbit of the outermost icy moon Callisto, can migrate using little or no fuel from orbits with large apoapses to smaller ones. This is shown in Figs. 1c and 1d in both the phase space and the inertial configuration space. From orbits slightly larger than Callisto's, the spacecraft can be captured into an orbit around the moon. The set of all capture orbits is a solid cylindrical tube in the phase space, as shown in Fig. 2a (for details of the tube computation, see, for example, [6]). Followed backward in time, this solid tube intersects transversely our Keplerian map, interpreted as a Poincaré surface of section. The resulting elliptical region, Fig. 2b, is an *exit* from Jovicentric orbits

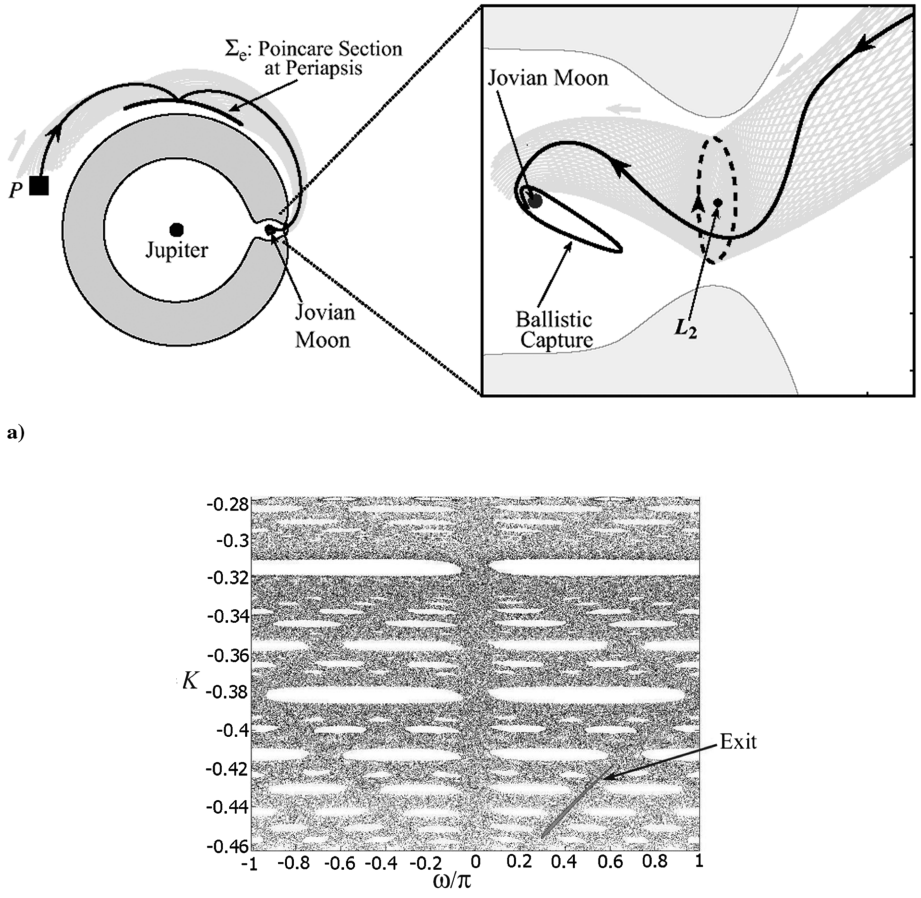

Fig. 2 Shown are the following. a) A spacecraft *P* inside a tube of gravitational capture orbits will find itself going from an orbit about Jupiter to an orbit about a moon. The spacecraft is initially inside a tube whose boundary is the stable invariant manifold of a periodic orbit about L_2. The three-dimensional tube, made up of individual trajectories, is shown as projected onto a configuration space. Also shown is the final intersection of the tube with Σ_e, a Poincaré map at periapsis in the exterior realm. b) The numerically computed location of an exit on Σ_e is shown, with the same map parameters as before. Spacecraft that reach the exit will subsequently enter the phase space realm around the perturbing moon. The vertical axis is the Keplerian energy *K* of the instantaneous conic orbit about Jupiter.

exterior to Callisto. It is the first backward Poincaré cut of the solid tube of capture orbits.

The advantage of considering an analytical two-dimensional map as opposed to full numerical integration of the restricted three-body equations of motion is that we can apply all the theoretical and computational machinery applicable to phase space transport in symplectic twist maps [10]. For example, previous work on twist maps can be applied, revealing the existence of lanes of fast migration between orbits of different semimajor axes. These lanes can be used by a spacecraft sent from Earth to the Jovian system. A spacecraft whose trajectory just grazes the orbit of the outermost icy moon Callisto can migrate using little or no fuel from orbits with large apoapses to smaller ones.

This Keplerian map is an approximate update map for the planar CR3BP; the approximation arises from fact that the kick function f is obtained by evaluating integrals while assuming an average value of K, that is, $\bar{K}$. An exact map can be obtained, but adds complication. A first attempt to derive an exact map was made by using the actual value K instead of an average value and mimicking the original procedure, that is, integrating the perturbation terms over an unperturbed orbit. But this resulted in additional derivative terms, and the resulting map did not turn out to be area preserving, a key property of the Poincaré map resulting from the full equations of motion that our map (1) has.

A second, more complicated way of deriving an exact map is to use the method of Hamilton–Jacobi, which has been developed for general Hamiltonian systems [11]. It involves a canonical change of variables, which leads to the elimination of perturbation in the time interval between two consecutive intersections with the Poincaré section. This procedure transforms the perturbed system into an integrable one for the interval between two periapes, and the evolution of transformed variables is then performed. The procedure involves a inverse canonical change of variables at the end of the period. The change of variables are given by generating functions that satisfy the Hamilton–Jacobi equations and can be solved to arbitrary orders of μ by perturbation theory for finite time intervals. An exact map was derived using this technique, but the implementation of the map is complicated; namely, we do not get a simple analytical expression for the map as we do in Eq. (1). The exact map derived this way, though interesting, does not have the simplicity we seek for preliminary mission design purposes.

III. Patched Three-Body Approximation

The P3BA discussed by Ross et al. [1] considers the motion of a spacecraft in the field of n bodies, considered two at a time, for example, Jupiter and its ith moon, M_i. When the trajectory of a spacecraft comes close to the orbit of M_i, the perturbation of the spacecraft's motion away from purely Keplerian motion about Jupiter is dominated by M_i. In this situation, we say that the spacecraft's motion is well modeled by the Jupiter–M_i spacecraft restricted three-body problem. For each segment of purely three-body motion, the invariant manifold tubes of L_1 and L_2 bound orbits (including periodic orbits) lead toward or away from temporary capture around a moon. The transport mechanism is associated with the dynamics of homoclinic and heteroclinic tangles, and the study of these dynamics leads to a general formulation of the transport in terms of distributions of small phase space regions called lobes [12].

Within the three-body problem, we can take advantage of phase space structures such as these tubes of capture and escape, as well as lobes associated with movement between orbital resonances. Both tubes and lobes, and the dynamics associated with them, are important for the design of an MMO trajectory. Portions of these tubes are "carried" by the lobes mediating movement between orbital resonances [6]. Directed movement between orbital resonances is what allows a spacecraft to achieve large changes in its orbit [1,9]. When the spacecraft's motion, as modeled in one three-body system, reaches an orbit whereby it can switch to another three-body system, we switch or "patch" the three-body model to the new system. This initial guess solution is then refined to obtain a trajectory in a more accurate four-body model. Evidence suggests that these initial guesses are very good [1], even in the full n-body model.

We now describe a methodology to obtain fuel-optimal trajectories for the MMO, with the help of the Keplerian map. During the intermoon transfer, in which one wants to leave a moon and transfer to another moon closer in to Jupiter, we consider the transfer in two portions, shown schematically in Fig. 3 with M_2 as the inner moon. In the first portion, the transfer determination problem becomes one of finding an appropriate solution of the Jupiter–M_1-spacecraft problem, which jumps between orbital resonances with M_1, that is, it performs resonant gravity assists to decrease the perijove [1]. M_1's perturbation is only significant over a small portion of the spacecraft trajectory near apojove (A in Fig. 3a). The effect of M_1 is to impart an impulse to the spacecraft, equivalent to a ΔV in the absence of M_1.

The perijove is decreased until it has a value close to the orbit of M_2, in fact, close to the orbit of L_2 of M_2. We can then assume that a gravity assist can be achieved with M_2 with an appropriate geometry, such that M_2 becomes the dominant perturber and all subsequent gravity assists will be with M_2 only. When a particular resonance is reached, the spacecraft can then be ballistically captured by the inner moon [6]. The arc of the spacecraft's trajectory at which the spacecraft's perturbation switches from being dominated by moon M_1 to being dominated by M_2 is called the "switching orbit." A rocket burn maneuver need not be necessary to effect this switch. The set of possible switching orbits is the "switching region" of the P3BA; see Fig. 4. It is the analog of the "sphere of influence" concept used in the patched-conic approximation, which guides a mission designer regarding when to switch the central body for the model of the spacecraft's Keplerian motion. A major difference is that the switching region is defined in the phase space and not just in the configuration space.

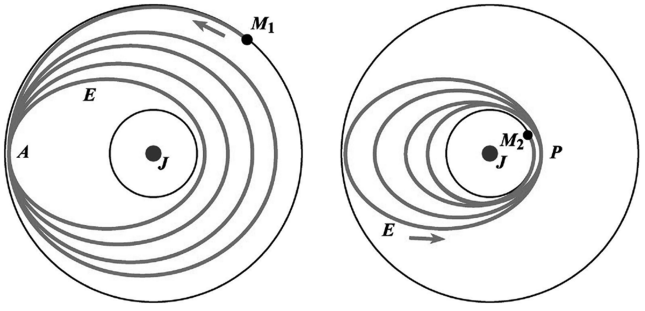

Fig. 3 Intermoon transfer via resonant gravity assists. a) The orbits of two Jovian moons are shown as circles. Upon exiting the outer moon's (M_1) sphere of influence, the spacecraft proceeds under third-body effects onto an elliptical orbit about Jupiter. The spacecraft gets a gravity assist from the outer moon when it passes through apojove (denoted as A). The several flybys exhibit roughly the same spacecraft/moon geometry because the spacecraft orbit is in near resonance with the moon's orbital period and, therefore, must encounter the moon at about the same point in its orbit each time. Once the spacecraft orbit comes close to grazing the orbit of the inner moon, M_2 (in fact, grazing the orbit of the L_2 point of M_2), the inner moon becomes the dominant perturber. The spacecraft orbit in which this occurs is denoted as E. b) The spacecraft now receives gravity assists from M_2 at perijove (P), at which the near-resonance condition also applies. The spacecraft is then ballistically captured by M_2.

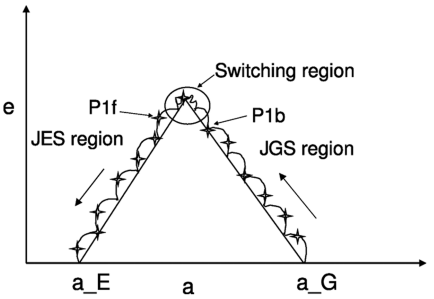

Fig. 4 Schematic trajectory in an a–e plane showing various regions. Various apoapses/periapses are marked with stars. The straight lines represent the constant three-body energy contours in the JGS and JES systems.

The task of searching for trajectories that go from near-Ganymede to near-Europa Jovicentric orbits can be simplified using the Keplerian maps for the two three-body systems. Given the size of the periodic orbit around L_1 of the Jupiter–Ganymede spacecraft (JGS) system, we can find its three-body energy. Similarly, given a target periodic orbit around L_2 of the Jupiter–Europa spacecraft (JES) system, we can find its three-body energy. The small neighborhood around the point at which the JGS and JES constant three-body energy contour lines intersect for a given set of energies represents the switching region. Figure 4 shows the various regions. The search for probable trajectories is done as follows:

1) We choose a point outside the switching region, lying on the JGS contour line and close to the switching region. Call it $P(=(a_0, e_0))$ and time $t = 0$. Without loss of generality, we assume the spacecraft is currently at (or close to) apojove. To uniquely define a trajectory in the four-body system, we need to specify the periapse angle with regard to the Jupiter–Ganymede (JG) line, ω_g, and with regard to the Jupiter–Europa (JE) line, ω_e, at time $t = 0$.

2) Now we want to choose the periapse angle with regard to the JG line so that the spacecraft gets a significant kick from Ganymede toward Europa and ends up in the switching region. Recall from the previous section that this implies the apoapse should occur with the periapse slightly more than $-\pi$ with regard to the JG line. Thus, we can narrow down the search space for ω_g at $t = 0$ to those values, that is, $-0.90\pi < \omega_g < -0.99\pi$.

3) The primary interaction with Europa occurs at periapse. Ideally, once the spacecraft gets the previously mentioned kick from Ganymede, we want it to get a further kick from Europa, toward Europa, at the following periapse. Again, recall that this implies the next periapse should occur with periapse slightly greater than zero with regard to the JE line. If we use only the planar CR3BP equations for the JGS system (i.e., put the mass of Europa to zero in the four-body equations) starting with time $t = 0$, ω_g selected from the aforementioned search space, and ω_e with an initial guess, we can find the periapse angle ω_e at the next periapse. Using predictor-corrector sensitivity analysis, we can refine the initial guess for ω_e at $t = 0$, so that the spacecraft gets a significant kick in the next periapse. Once we have a range of values of ω_e at $t = 0$ that give the desired phase for the next few periapses, we can use full four-body equations to determine the actual trajectory in the switching region. The narrowed-down search space for ω_e and ω_g is labeled S_ω. Recall that the path of the spacecraft in this region is called the switching orbit. The first forward iterate at periapse into the JES region is labeled $P1_f$ and the first back iterate at apoapse into the JGS region is labeled $P1_b$. Note that, if in step 1 the point is chosen exactly at apoapse, then $P1_b = P$.

4) Now we need to search for the conditions from the set S_ω that will lead to a successive decrease in the semimajor axis when iterated forward and an increase in the semimajor axis value when iterated back, outside the switching region. This task of iterating in the JES and JGS regions can be efficiently handled by the Keplerian maps. For each pair (ω_g, ω_e) and a point $P(a_0, e_0)$ in the switching region, we iterate forward the corresponding point $P1_f$ using the periapse map, which is valid only in the JES region, and iterate backward the

corresponding point $P1_b$ using the apoapse map, which is valid only in the JGS region.

5) Once we have found which values among the set S_ω will result in a Jovicentric orbit from near Ganymede to near Europa using the separate Keplerian maps, we use the full four-body equations to get actual trajectories. In some cases, because the maps are not exact, the trajectories and transfer times obtained by the full four-body equations differ significantly from those obtained from the maps. But we do get a number of topologically different trajectories by using maps that are verified by full four-body equations. We can also cycle through various nearby (a, e) values in the switching region to get appropriate trajectories.

We show an actual trajectory for the four-body system obtained by using the method described in Fig. 5. Figure 5a shows the semimajor axis time history, starting from the exit from Ganymede to capture by Europa. Figure 5b shows the time history in an a–e plot, clearly showing that the spacecraft closely follows the constant energy contours in the two regimes. Figures 5c and 5d show the three-body energy history of the spacecraft for the Jupiter–Ganymede and Jupiter–Europa spacecraft systems. The two solutions were patched together and the switching region, in which the switching of the dominant perturber occurs in the actual four-body trajectory, is marked. Clearly, the three-body energy for the JGS system is constant before the switching region, and the energy for the JES system is almost constant after the switching region. This separation of domains of influence of the two perturbers suggests that the patched three-body approach can be used to obtain good initial guesses for the actual trajectory, which can in turn be obtained by using the four-body equations. Hence, we can use two separate Keplerian maps and patch the solutions appropriately to get initial guesses.

The trajectory shown in Fig. 5 has a very long transfer time between the two moons, arising primarily due to the spacecraft getting stuck in a resonance for a very long time. To overcome this problem and to design fuel-efficient trajectories with realistic transfer times, we introduce the controlled Keplerian map in the next section.

IV. Method for Designing Trajectories Using Controlled Map

The controlled Keplerian map with a control u is an update map for the angle of periapse (or apoapse) ω in the rotating frame and Keplerian energy K, F: $\mathcal{A} \times U \to \mathcal{A}$

$$F\left(\begin{pmatrix}\omega_n\\ K_n\end{pmatrix}, u_n\right) = \begin{pmatrix}\omega_{n+1}\\ K_{n+1}\end{pmatrix} = \begin{pmatrix}\omega_n - 2\pi\{-2[K_n + \mu f(\omega_n) + \alpha u_n]\}^{-3/2}\\ K_n + \mu f(\omega_n) + \alpha u_n\end{pmatrix} \tag{2}$$

where $u_n \in U = [-u_{\max}, u_{\max}]$, $u_{\max} \ll 1$. The term $\alpha = \alpha(C_J, \bar{K})$ is approximated as constant. The control strategy employed to get desired trajectories is twofold. It involves a coarse control part in which the aim is to get a rapid decrease in the semimajor axis value of the spacecraft and a fine control part, in which we target specific regions of interest in the phase space. The reason for this two-pronged strategy is that the traditional forward–backward approach [13] works best only if there are no big resonances in between the starting point and the target region. If the source and target regions lie in two distant regions separated by slow transport barriers, then the time before an intersection takes place in this approach is very large. During that time, the extensions of both the image of the source segment and the preimage of the target segment grow exponentially in size, which requires an exponentially increasing number of discrete points to resolve them. As was mentioned earlier and is evident from Fig. 1b, the phase space for our problem is populated with big resonances resulting in a mixed phase space; hence, the

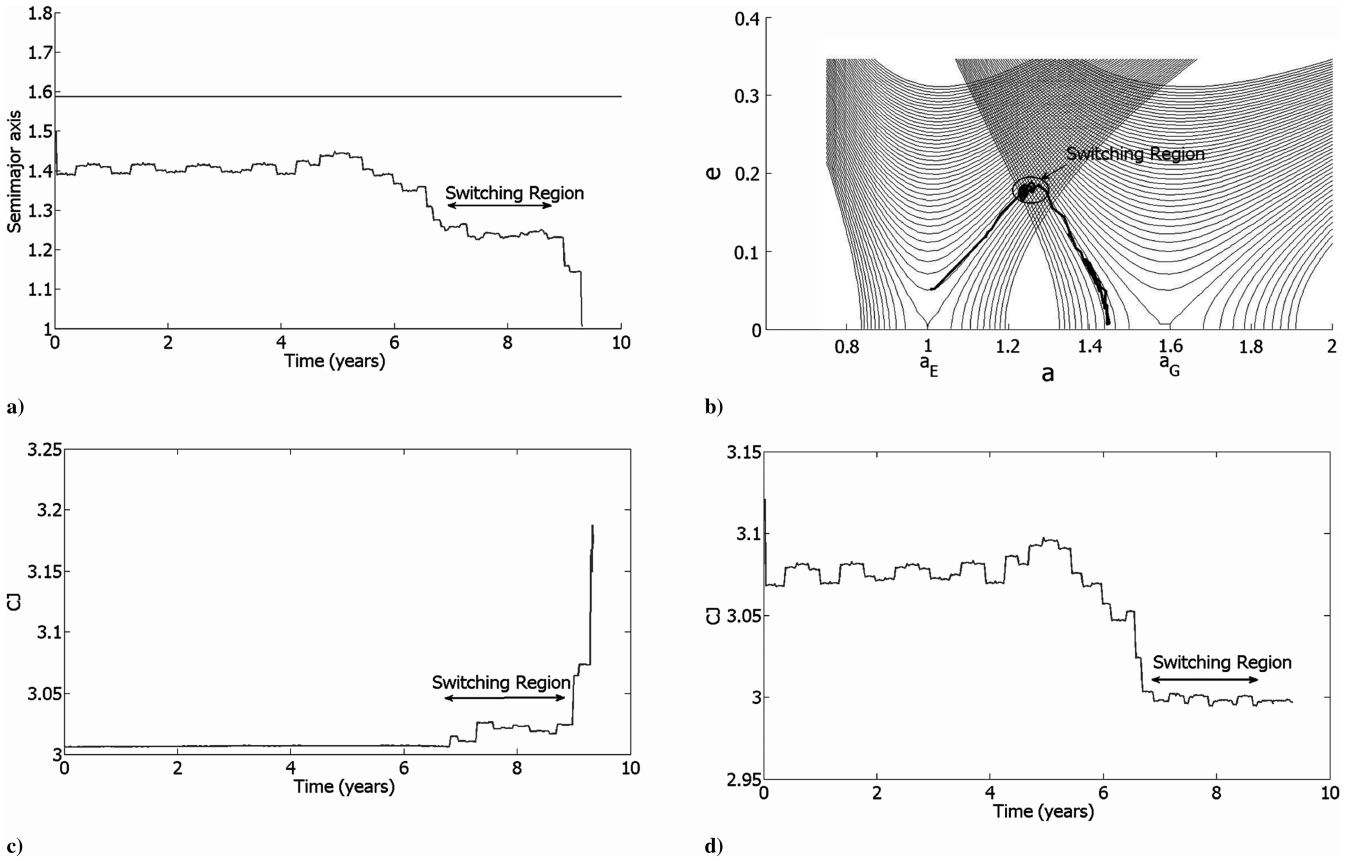

Fig. 5 Trajectory found using the patched three-body approximation: a) semimajor axis time history, b) trajectory in the a–e plane, c) Jacobian constant for the JGS system, and d) Jacobian constant for the JES system. The trajectory was obtained by integrating the full four-body system.

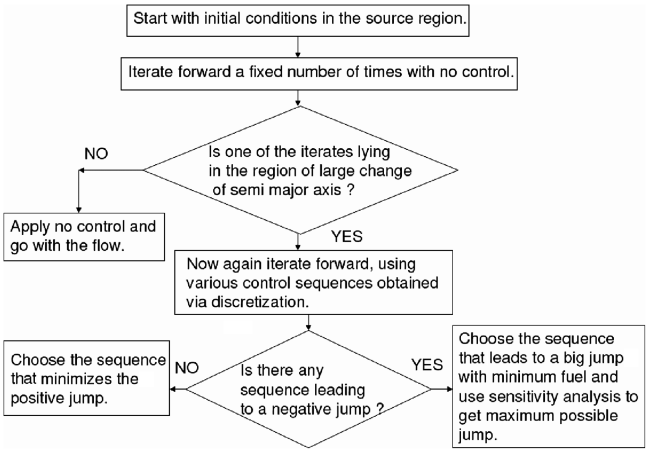

Fig. 6 The coarse control algorithm.

forward–backward approach alone would not be sufficient for our purposes. The coarse control algorithm is based on the fact that large changes in the semimajor axis (i.e., the action) occur for a very small range of values of the periapse angle (i.e., the angle); see Fig. 1a. We adopt the policy of "going with the flow," until we approach a region in which there is going to be a large change in the semimajor axis. The outline of the algorithm for a single three-body system is as follows and is also shown in Fig. 6.

1) At (ω_n, a_n), we iterate forward $n_{\max}$ steps with $u = 0$, where $n_{\max}$ holds an inverse relationship with $u_{\max}$. If any of the calculated iterates lies with the region of high increase, labeled A_+, or the region of high decrease, labeled A_-, we calculate the control (Figs. 2a and 2b, respectively). Otherwise, we do not employ any control at the current iteration step (i.e., $u_n = 0$). The size of both these regions (i.e., A_- and A_+) is directly proportional to the parameter $\delta\omega$.

2a) Ideally, if one of the future iterates that have been calculated is in A_+, we want to apply control so as to move the iterate away from it to the neighboring A_- region. If the ith iterate (where $i < n_{\max}$) is in A_+, we calculate a control sequence over the next i iterates. The control domain (i.e., $[-u, u] \times [-u, u] \times \cdots i$ times) is coarsely discretized, and we obtain the iterates using each control sequence resulting from the discretization. Computations in this paper were done using a discretization equivalent to ΔV of 1 m/s, and $u_{\max}$ was taken as equivalent to ΔV of 5 m/s, in either direction. If there are some sequences that result in the final iterate being in A_-, we choose the sequence that results in the final iterate being in a small neighborhood of ω_{opt}. Here, ω_{opt} is the value of ω that leads to the maximum decrease in the semimajor axis over one iteration. Then, using a sensitivity analysis with regard to the control at the last nonzero iterate in the chosen control sequence, we can adjust its value so that the resultant $\omega \approx \omega_{\text{opt}}$; hence, we get the maximum possible kick in the desired direction.

On the other hand, if there is no such sequence that results in the final iterate being in A_-, we need to move the final periapse angle in the other direction so as to minimize the increase in a. This local optimization can be handled by a similar discretization procedure as already mentioned.

2b) If one of the future iterates is in A_-, we again use the aforementioned discretization of the control domain and choose the control sequence in the same way as before. A sensitivity analysis is used to get the final $\omega \approx \omega_{\text{opt}}$.

3) Once a threshold value of a is reached, we switch to fine control. Fine control can be handled by the forward–backward method, in which the target is the interior of the first intersection of the stable invariant manifold of a periodic orbit around L_2 with the Poincaré section at periapse.

In Fig. 7, we show a sample trajectory obtained by the aforementioned algorithm for the Jupiter–Europa spacecraft system. Note that, as a result of appropriately timed control inputs, the spacecraft visits the region of high decrease of the semimajor axis.

We can now use this algorithm within the framework of a patched three-body approximation. We use the controlled apoapse map to get the trajectory from near Ganymede to the switching region and then patch it with another trajectory obtained by using a controlled periapse map, which leads to capture around Europa. A sample trajectory for such a case is shown in Fig. 8. The spacecraft completes this trajectory using 160 m/s of fuel in 1.7 years, which includes 116 revolutions around Jupiter (periapse/apoapse passages). The time taken for this mission is less than 10% of that taken for the optimal (zero) fuel trajectory for the same four-body system shown earlier. Also, this framework is an improvement over the methods that involve large ΔV [14] and is a more complete method of designing trajectories in a four-body system than using some variant of the traditional patched conics approach [15].

For the sake of completeness, we briefly discuss the tradeoff issues between the time of flight and fuel (control), because such a tradeoff is typically discussed in all low-fuel mission design frameworks. The amount of fuel used for providing ΔV is expected to be proportional to the parameter $\delta\omega$ up to a saturation point, because this parameter decides the size of the region in the phase space in which the control is actively applied, as discussed earlier. More proactive control is also expected to decrease the time of flight up to a certain limit. In Fig. 9, we show plots illustrating the time of flight vs fuel tradeoff for a single three-body system (Jupiter–Europa spacecraft). Several random initial conditions were taken near $a = 1.5$, and we show the plots for two of those conditions that take the most (upper line) and the least (lower line) amount of iterations to reach the exit region for three different values of $\delta\omega$. The basic characteristics of this system are expected to be similar for patched three-body systems.

There are a few implementation issues that need to be discussed. There is no known optimal way to chose values for the parameters $n_{\max}$ and $\delta\omega$ for the algorithm. We selected $n_{\max} = 5$ for our simulations, which provided a reasonable compromise between computational time and adequate results. With more computational resources, a higher value can be used to obtain slightly more fuel-efficient trajectories for a given time of flight (up to the theoretical optimum).

If a low value of $\delta\omega$ is chosen, leading to less proactive control, then there is a chance of the spacecraft getting stuck in resonance

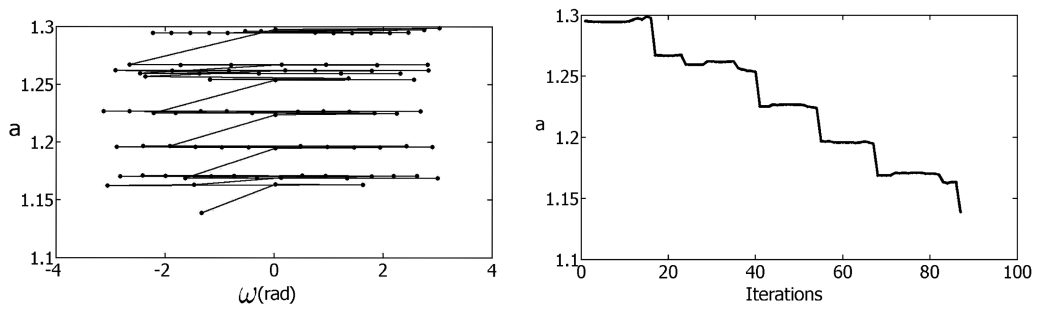

Fig. 7 Sample trajectory designed using the algorithm: a) plot of the semimajor axis vs periapse angle, and b) time history of the semimajor axis. The spacecraft repeatedly visits the region of large decrease in the semimajor axis.

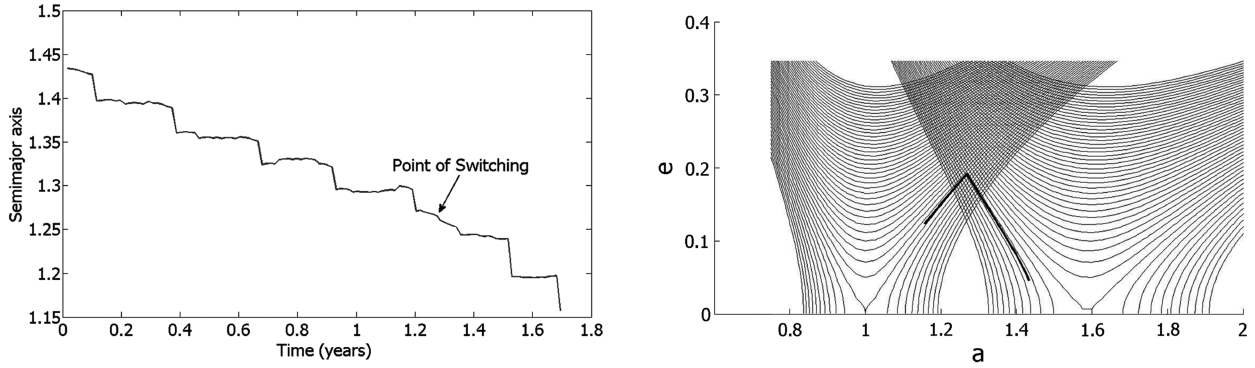

a) b)

Fig. 8 Trajectory for the Jupiter–Europa–Ganymede system using the patched three-body approach: a) time history of the semimajor axis, and b) semimajor axis vs eccentricity plot with three-body energy contours lines in the background.

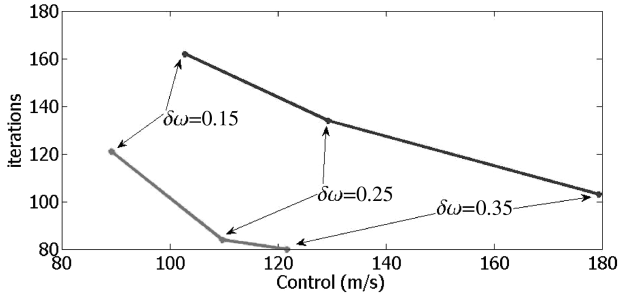

Fig. 9 Plot showing the tradeoff between control used and number of iterations required for two different initial conditions leading to capture around Europa for the Jupiter–Europa spacecraft planar CR3BP.

regions for long times. Hence, we used a check in the program, which will increase the $\delta\omega$ for a small duration if such a case is detected.

V. Conclusions

With the help of a family of analytical two-dimensional Poincaré maps, exact uncontrolled trajectories in the full equations of motion of the four-body Jupiter–Europa–Ganymede spacecraft system were found. The maps were used for fast propagation in regimes in which one of the two perturbers is dominant. Additionally, the maps reduced the patching region search space, that is, the search for the region in which the perturbers have comparable influence, given by critical values of the spacecraft phase with regard to the Jupiter–Ganymede and Jupiter–Europa systems. The fast propagation done by the maps on either side of the patching region made preliminary trajectory generation faster than integrating the full equations of motion. Many of the trajectories obtained using the algorithm were topologically similar to those finally obtained by full integration (i.e., the same number of orbits around Jupiter). The fact that the two three-body energies were almost constant in the actual four-body trajectory on either side of the patching region 1) gives us confidence that there exist actual trajectories that shadow those obtained with the help of the maps, and 2) implies a separation of regimes of influence of the perturbers. The relationship between trajectories found via the maps and trajectories in the full n-body equations of motion needs to be investigated further to make the qualitative analysis given here more applicable to actual implementation for mission design.

Taking note of the apparent validity of the patched three-body approach and the utility of the Keplerian maps, we used those Keplerian maps to derive approximate controlled trajectories in the four-body system. Depending upon the chosen value of the parameter of the algorithm, a compromise can be reached between the amount of fuel used and the time taken to complete the mission. We believe that the numbers so obtained should give us a first-order estimate of fuel required for actual trajectories in full four-body systems, although this needs to be verified by further investigations.

The use of multiple gravity assists and algorithms such as those mentioned in this paper are stepping stones toward automating the design process of various complicated missions envisioned for the future. This is a significant improvement over the methods that involve large ΔV and is a more complete method of designing trajectories in a four-body system than using the patched conics approach.

The maps used in both the algorithms are two-dimensional maps, primarily because the system we considered, the Jupiter–Europa–Ganymede system, is a very nearly coplanar system; hence, the dynamics involved for a spacecraft restricted to this plane occur in 2 degrees of freedom. This approach can further be extended to model a 3-degree-of-freedom motion, resulting in four-dimensional maps, the two additional dimensions being inclination i and the longitude of the ascending node Ω. The use of four-dimensional maps may uncover some exotic trajectories, although the implementation will be difficult because the search space will be larger due to the increase in dimensions.

The algorithm mentioned for finding appropriate control inputs can also be used in any physical modeling problem in which the dynamics are similar to those described by this Keplerian map. The main characteristic of this map is that the kick is significant for only a small range of values of an angle; hence, by using appropriate control inputs obtained by this algorithm, a particle can be made to have the desired large changes in the corresponding action.

Appendix: Mathematical Description of the Kick Function

The kick function $f(\omega)$ is given by

$$f(\omega) = -\frac{1}{\sqrt{p}}\left[\left(\int_{-\pi}^{\pi}\left(\frac{r}{r_2}\right)^3 \sin[\omega + \nu - t(\nu)]\,\mathrm{d}\nu\right) - \sin\omega\left(2\int_0^{\pi}\cos[\nu - t(\nu)]\,\mathrm{d}\nu\right)\right]$$

where

$$r = p/(1 + e\cos\nu) \qquad p = a(1 - e^2) \qquad a = -1/(2K)$$

$$r_2 = \sqrt{1 + r^2 - 2r\cos\theta} \qquad \theta = \omega + \nu - t(\nu)$$

and the relationship between the true anomaly ν and time t is obtained through Kepler's equation. It appears initially that f is a function of ω, K, and e. But the invariance of the Jacobian constant yields a relationship between these three variables, implying $f = f(\omega, K; C_J)$, where C_J is a parameter. Furthermore, if we assume K is constant, at a value $\bar{K}$, then this also becomes a parameter and f is a function of ω only, that is, $f(\omega) = f(\omega; C_J, \bar{K})$ with both C_J and $\bar{K}$ considered as constant parameters.

References

[1] Ross, S. D., Koon, W. S., Lo, M. W., and Marsden, J. E., "Design of a Multi-Moon Orbiter," American Astronomical Society Paper 03-143, Feb. 2003.

[2] Whiffen, G. J., "An Investigation of a Jupiter Galilean Moon Orbiter Trajectory," American Astronomical Society Paper 03-544, Aug. 2003.

[3] Ross, S. D., "The Interplanetary Transport Network," *American Scientist*, Vol. 94, 2006, pp. 230–237.

[4] Conley, C. C., "Low Energy Transit Orbits in the Restricted Three-Body Problem," *SIAM Journal on Applied Mathematics*, Vol. 16, 1968, pp. 732–746.
doi:10.1137/0116060

[5] Belbruno, E. A., and Miller, J. K., "Sun-Perturbed Earth-to-Moon Transfers with Ballistic Capture," *Journal of Guidance, Control, and Dynamics*, Vol. 16, 1993, pp. 770–775.
doi:10.2514/3.21079

[6] Koon, W. S., Lo, M. W., Marsden, J. E., and Ross, S. D., "Heteroclinic Connections Between Periodic Orbits and Resonance Transitions in Celestial Mechanics," *Chaos*, Vol. 10, 2000, pp. 427–469.
doi:10.1063/1.166509

[7] Koon, W. S., Lo, M. W., Marsden, J. E., and Ross, S. D., "Low Energy Transfer to the Moon," *Celestial Mechanics and Dynamical Astronomy*, Vol. 81, 2001, pp. 63–73.
doi:10.1023/A:1013359120468

[8] Belbruno, E., *Capture Dynamics and Chaotic Motions in Celestial Mechanics: With Applications to the Construction of Low Energy Transfers*, Princeton Univ. Press, Princeton, NJ, 2004.

[9] Ross, S. D., and Scheeres, D. J., "Multiple Gravity Assists, Capture, and Escape in the Restricted Three-Body Problem," *SIAM Journal on Applied Dynamical Systems*, Vol. 6, No. 3, 2007, pp. 576–596.
doi:10.1137/060663374

[10] Meiss, J. D., "Symplectic Maps, Variational Principles, and Transport," *Reviews of Modern Physics*, Vol. 64, 1992, pp. 795–848.
doi:10.1103/RevModPhys.64.795

[11] Abdullaev, S. S., *Construction of Mappings for Hamiltonian Systems and Their Applications*, Springer, New York, 2006.

[12] Dellnitz, M., Junge, O., Koon, W. S., Lekien, F., Lo, M. W., Marsden, J. E., Padberg, K., Preis, R., Ross, S. D., and Thiere, B., "Transport in Dynamical Astronomy and Multibody Problems," *International Journal of Bifurcation and Chaos in Applied Sciences and Engineering*, Vol. 15, 2005, pp. 699–727.
doi:10.1142/S0218127405012545

[13] Shinbrot, C. G. T., Ott, E., and Yorke, J., "Using Chaos to Direct Trajectories to Targets," *Physical Review Letters*, Vol. 65, 1990, pp. 3215–3218.
doi:10.1103/PhysRevLett.65.3215

[14] Koon, W. S., Lo, M. W., Marsden, J. E., and Ross, S. D., "Constructing a Low Energy Transfer Between Jovian Moons," *Contemporary Mathematics*, Vol. 292, 2002, pp. 129–146.

[15] Strange, N. J., and Longuski, J. M., "Graphical Method for Gravity-Assist Trajectory Design," *Journal of Spacecraft and Rockets*, Vol. 39, 2002, pp. 9–16.
doi:10.2514/2.3800